Material Removal of Hip Stem Prosthesis Using Bio-Inspiration from Trabecular Bone

Mathieu Bilhère-Dieuzeide, Julien Chaves-Jacob, Emmanuel Buhon, Guillaume Biguet-Mermet, Jean-Marc Linares

Available online at www.sciencedirect.com

ScienceDirect

Procedia CIRP 110 (2022) 267–272

www.elsevier.com/locate/procedia

V CIRP Conference on Biomanufacturing

Material Removal of Hip Stem Prosthesis Using Bio-Inspiration from Trabecular Bone

Mathieu Bilhère-Dieuzeide[a,b], Julien Chaves-Jacob[a,*], Emmanuel Buhon[b], Guillaume Biguet-Mermet[b], Jean-Marc Linares[a]

[a] *Aix-Marseille Univ, CNRS, ISM, Inst Mouvement Sci, UMR 7287, Marseille, France*
[b] *Thales LAS (Land Air System) France OME (Optronics and Missile Electronics), Elancourt, France*

* Corresponding author. Tel.: +33413946277. *E-mail address:* julien.chaves-jacob@univ-amu.fr

Abstract

In the hip stem prostheses domain, stress shielding represents a major issue due to its potential implant loosening effect. This phenomenon occurs when the implant is much stiffer than the bone itself. A way to reduce this stiffness difference is to remove material from the implant. In addition, this solution leads to mass reduction of the implant, improving the patient quality of life. To insure the implant will withstand the loading, material must be distributed in a specific way. Bones use the same objectives of lightness and mechanical efficiency while using a minimal amount of material. In addition, these biological structures are well spread and reliable in living beings, especially in mammals and avian species. In this paper, a method bio-inspired by trabecular bone structure is proposed to remove material from parts considering their mechanical stress field. In Nature, trabecular bone is defined as a graded porous material with bone material locally oriented along the local stresses' direction. To mimic this natural behavior, the proposed method generates local porosities bio-inspired in position, shape, size and orientation. To evaluate the proposed method performance, experimental tests were carried out on a hip prosthesis stem. Test results demonstrated that the method can be used to reduce the stiffness of the prosthesis while withstanding the applied constrains.

Keywords: Biologically inspired design ; Design optimization ; Trabecular bone ; Lightweight structures ; Finite Element Analysis

1. Introduction

Prostheses are well known and studied for many years [1] and are ones of the most widely implanted prostheses on the market. They have been created to restore the continuity of the broken structure in order to maintain the quality of living of the patient [2]. The most common material used for hip implant is titanium [3] due to its biocompatibility. This material has high mechanical strength and is lightweight [2]. However, it presents a high Young's modulus (E), so a high stiffness which can be damaging. Indeed, implant loosening may appear if the difference of stiffness between the bone and the implant is too large [4]. In this case, the implant absorbs all the loadings while the bone is unloaded. For this reason, bone resorption is predominant in the surrounding of the implant during the bone turnover process [5]. This lack of material formation causes a loss of adherence between the implant and the bone: it is the "stress shielding" [6]. It is manifested by problems of implant loosening and results in failure of the implant.

For titanium implants, the implants are about nine times stiffer than the bone itself ($E_{titanum} \approx 110GPa$ while $4GPa < E_{bone} < 30GPa$) [7]. To reduce the risks of stress shielding, the difference of stiffness between the bone and the implant has to be reduced [4]. In this way, a more homogeneous assembly {implant; bone} is created and loadings are more evenly

2212-8271
10.1016/j.procir.2022.06.048

distributed. Finally, stresses induced into bone are higher and bone formation can occur. To achieve this stiffness reduction (while insuring the implant can withstand the loadings of the daily life of the user), the geometry of the implant can be modified. To fulfill this optimization problem, some classic solutions are already proposed in the literature. Topology optimization is the most used solution for optimization [6]. It consists in finding the best material distribution within a fixed domain with precise boundary conditions. Using this method, the geometry of the studied part would be oriented along the stresses direction. It can be macro-scale or multi-scale optimization [8]. To fulfill optimization problems, lattice structures are also often used. These structures soften the implant and give mechanical properties closer to the bone ones in compression [4]. Also, these structures can be graded: the thickness of the struts depend on the local stresses. These structures are a step toward porous implants which have biocompatibility advantages favoring tissue ingrowth [9]. If porosities are graded, large pores insure damping functions while small pores insure bone tissue ingrowth [9]. Organic matter flows into the implant porosities as in bone porosities and colonize the implant to create a stronger linkage between the two entities [10]. Due to their "material removal" definition, all these three solutions provide lighter prosthesis that make users' life easier.

The proposed method of material removal is stress-driven and bio-inspired by trabecular bone structure. This method will remove material from a part, thus reduce its mass and so decrease its stiffness, ensuring it can withstand the loadings it is designed for. The removal process is insured by adding holes in the part that are bio-inspired in position, shape, orientation and size. In Section 3, this method will be applied on a hip stem prosthesis. The stiffness of the initial and bio-inspired prostheses will be compared. In a second bio-inspired prosthesis design, biocompatibility will be more taken into account.

2. Mass reduction method

This section will focus on the study of bone structure and the derived bio-inspired laws used in the method. The end of the section will present the method [11, 12].

2.1. Bone structure

The method is based on long bone from mammal's endoskeletons. Indeed, it appears that they undergo loads similar to conventional mechanical loads (bending, compression, etc.) [13]. More precisely, the method is based on epiphysis region of the bone, made of trabecular bone. It is described as porous bone that consists in an assembly of walls, called trabeculae, separated by void spaces called porosities [14].

These trabeculae (or trabecular walls), and so the surrounding porosities, are arranged in a specific way so that they can support high loads using a limited amount of material [15]. The trabecular structure follows the commonly used and named Wolff's law. It states that local bone structure is adapted from the local mechanical stress field induced by the loadings that the bone undergoes [16]. The bigger the stresses, the denser the bone and so the thicker the walls (and the smaller the porosities) and vice versa [17]. Commonly, the thickness of the walls is named "trabecular thickness" (noted Tb_{th}) and the size of the porosities is named "trabecular separation" (noted Tb_{sp}) (Fig. 1a) [18].

In addition, bone presents an anisotropic mechanical behavior. This behavior is locally represented by an ellipsoidal fabric tensor [19] oriented along the principal local mechanical stresses. It means that the trabeculae possess a specific orientation, so do the porosities, depending on the orientation of the principal mechanical stresses. This orientation favors the bone mechanical performances.

While nature focuses on bone turnover (creation and removal), the proposed method focuses on the porosities, so on material removal.

2.2. Bio-inspired laws

Wolff's law is the basis of many long bone trabecular structure based bio-inspiration. Locally, the bone volume fraction v_f (also named "bone density") depends on the stress field. To translate this link to a mechanical purpose, a law has been proposed to relate the local bone volume fraction v_f with the local Von Mises stresses σ_{VM} normalized by the bone yield strength Re [11]. This power law is used to determine the necessary local volume fraction v_f.

In addition, Tb_{th} and Tb_{sp} depend on the studied species (in the animal rein) [20]. More generally, these parameters are linked with the considered specie, the size of the specimen and its mass. Thus, a link has been proposed to relate the characteristic lengths of trabecular bone (Tb_{th} and Tb_{sp}) with the characteristic length of the bone itself, the femoral head diameter of the mammal and avian families [11].

2.3. Bio-inspiration process

The previously presented laws are the core of the bio-inspired method [11]. In this section will be presented the bio-inspiration process used to locally remove material of a part to reduce the amount of used material limiting the decrease of mechanical performances.

First, based on the ellipsoidal shape of the fabric tensor (Section 2.1), the used porosities will be ellipses (Fig. 1b).

The second step is to define the pattern used to discretize the part. It mimics the link between $\{Tb_{th}; Tb_{sp}\}$ and the femoral head diameter (Fig. 1b). The chosen pattern is a Faced Centered Cubic (FCC) of side length "pattern size" p. It is composed of independent elliptic porosities distributed as shown in Fig. 1b. While p mimics the Tb_{th}+Tb_{sp} parameter, the femoral head diameter is mimicked by the characteristic length of the part. As in the bone structure, the ellipses are independently aligned along the local principal stresses direction. The remaining material will then be aligned with the principal stresses similarly to the trabeculae in the bone. The ellipses are defined by three groups of parameters: their

position (abscissa and ordinate defined by the discretization using the pattern size p), their dimensions (semi-major and minor axis length, respectively a and b) and their orientation (Fig. 1b).

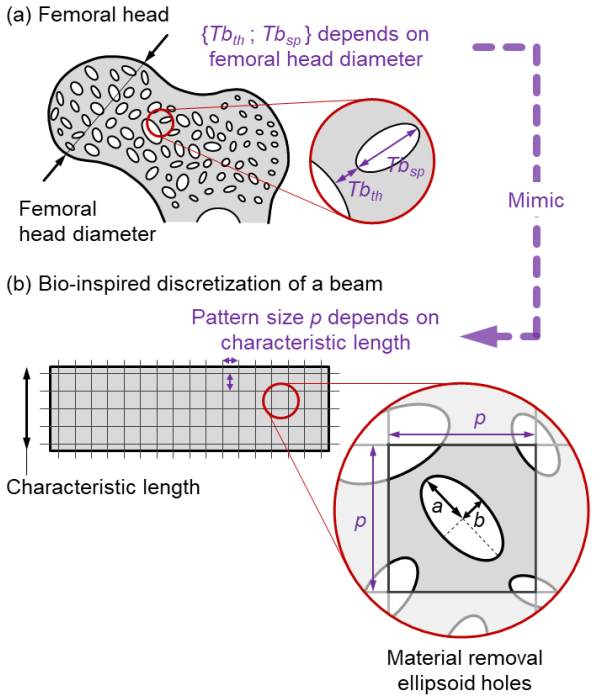

Fig. 1. Schema of the femoral structure (a) used to develop the bio-inspired discretization applied on a beam (b)

The third step is to determine the local material volume fraction v_f. This data can be determined using the law linking v_f with σ_{VM}/Re (Section 2.2) adapted to the part. A threshold is set to insure material cohesion in the part.

The fourth step is the dimensioning of the ellipses. For this aim, a link is highlighted between the ratio of the semi-axis lengths of the ellipses (a and b), named the "form factor" FF (equal to a/b) and the principal stresses ratio (equal to σ_1/σ_2 in 2D) [11, 21]. Mixing the parameters p, v_f and FF, the semi-axis lengths of the ellipses can be found.

3. Application case: hip prosthesis

This section will focus on the study case: a hip prosthesis stem. First, the design of the initial part will be presented; second, the material removal process will be detailed; to conclude the section, experimental validation will be presented.

3.1. Design of the hip prosthesis

The material removal process is applied on a hip stem prosthesis, called the Initial Prosthesis (IP) in the following. Its design is based on implants of the market. The main characteristics of a hip prosthesis are integrated in the IP: the stem/femoral neck angle of 135° [22] and the angle of the application of the forces for testing of 10° [23]. Then, since many shapes and sizes are marketed, the design of the IP depends on the standards used. Here a 12mm diameter prosthesis is designed (Fig. 2a).

3.2. Hip prosthesis material removing

Based on Section 2.3, the first step of the material removal process is to determine the stress field in the IP using Finite Element Analysis (FEA). The proper functioning of the process depends on the quality of the FEA and more precisely on the quality of the obtained stress field, so on the defined boundary conditions. A computational homogenization could have been considered [24] but due to the size gradient of the porosities (Fig. 2b), a traditional macroscopic FEA is preferred. The considered boundary conditions are based on ISO7206-3 standard certification fatigue cycles [23] adapted to a 2D static problem (presented in Section 3.3.1).

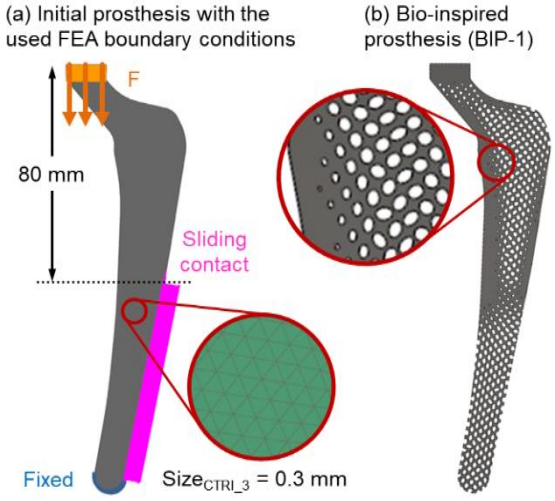

Fig. 2. Presentation of the initial hip prosthesis (IP) with the FEA boundary conditions and parameters applied during the whole study (a) / First bio-inspired prosthesis (BIP-1) obtained through the material removal process (b)

The bio-inspiration process led to the Bio-Inspired Prosthesis (BIP-1) presented in Fig. 2b. The chosen pattern size p_1 had been oversized compared to the pattern size computed with the bio-inspired laws. It allows to reduce drastically the stiffness of the implant and to get thicker walls between porosities. Finally, in the numerical simulation, 29% of material has been removed from the initial prosthesis IP. It also has been validated that the prosthesis BIP-1 would be safe to use according to the set of boundary conditions. Indeed, stresses due to the applied forces are smaller than the Ti6Al4V yield strength (criterion used in [25]). In addition, stresses are smaller than one third of the yield strength, so the part should be able to withstand fatigue cycles.

3.3. Experimental validation

This section will focus on the experimental validation of the material removal process. First, the BIP-1 will be numerically compared with the IP. Second, testing will be carried out to compare the BIP-1 with the IP. Finally, a

second bio-inspired prosthesis BIP-2 will be designed and will be compared with the IP and the BIP-1.

3.3.1. FEA on BIP-1

In his sub-section, the IP and BIP-1 will be compared through FEA simulations. For the simulations, the boundary conditions used in Section 3.2 will be imposed on the FEA model. These boundary conditions are set to match the experimental testing ones (Section 3.3.2). They are determined and adapted from the ISO7206-3 standards certifications. The lower part of the prosthesis will be fixed [26] while a part of the right side will present a sliding contact. The top 80mm of the prosthesis is free to move [23] and only subjected to a force corresponding to stumbling $F_{stumbling}$. This force is represented by a compression force along the gravitational direction (Fig. 2a) [25]. $F_{stumbling}$ causes a displacement that will be compared for both prosthesis (Fig. 3). It will give an idea of the relative stiffness of the parts.

The applied forces correspond to stumbling of a m=90kg person. In the standard certifications, the forces are defined as percentages of body weight. Averaging data from [27, 28], $F_{stumbling}$ is about 793% of body weight and forces due to stumbling are about 7000N (Eq. 1).

$$F_{stumbling} = 793\ \%BW = \frac{m * g * 793}{100} \quad (1)$$

For the FEA, the material set is titanium alloy Ti6Al4V (one of the most used material for hip prosthesis) and the mesh used is a thin shell mesh of 0.3mm linear triangles (Fig. 2a).

The FEA results are shown in Fig. 3. It appears that for a same applied force, the displacement observed on the BIP-1 are bigger than the one of the IP. The BIP-1 appears to be 22% softer than the IP. This comparison has been made possible because stresses are smaller than the Yield strength of Ti6Al4V and thus the strain and the stress in the material are still linearly related.

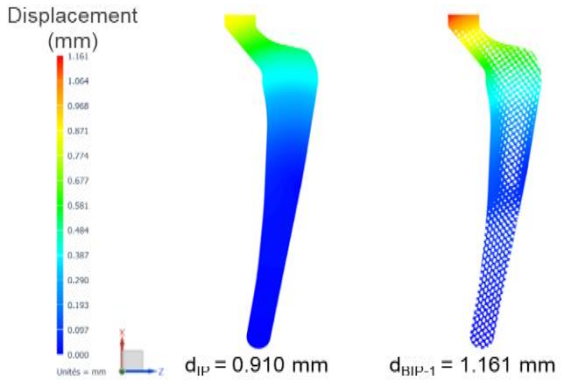

Fig.3. Displacement field induced in the initial prosthesis (IP) compared to the displacement field induced in the bio-inspired prosthesis 1 (BIP-1)

3.3.2. Experimental test

The two prosthesis have been printed with plastic material and then compared onto the same test bench (presented in Fig. 4). As introduced in previous sub-sections, the experimental test consists in compression of the prosthesis following a process adapted from ISO7206-3 standards certifications.

In this study case, the problem had been simplified to a 2D static problem: the applied compressive force was purely vertical. The prosthesis is placed into a supporting block in a locked vertical position. On the top side of the prosthesis, a displacement is imposed to generate the reaction force that is measured by a multicomponent dynamometer.

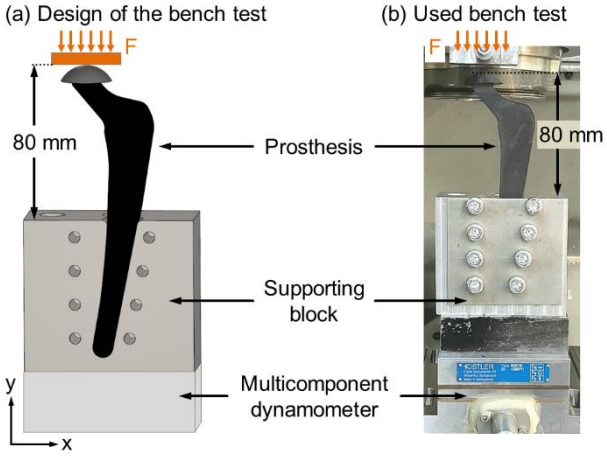

Fig. 4. Experimental benches

The prostheses were 3D printed using plastic material: a 31% mass reduction has been measured from the IP to the BIP-1 (similar to the 29% material removed by the process in theory). Due to the use of this plastic material, force scaling has to be done. Also, the critical force that can cause lamination $F_{lamination}$ of the prosthesis has to be calculated. For this aim, it is important to recall that in the FEA simulations on titanium prostheses, the stresses were much smaller than the titanium yield strength. For that reason, the prosthesis were loaded in the elastic range of the material. In this range, cross multiplications can be used to determine $F_{lamination}$. Knowing the materials yield strength and the stresses generated by a force on the titanium prosthesis, $F_{lamination}$ can be estimated. In this case, $F_{lamination}$ is estimated to 1200N. During the tests, the applied forces were lower than $F_{lamination}$, so no lamination should occur and the prostheses were loaded in the elastic range of the material.

In Fig. 5, the reaction force of the prostheses has been plotted as a function of the imposed displacement, for both the IP and the BIP-1. It can be observed that the BIP-1 is 25% less stiff than the IP.

It can be conclude that regarding the stiffness, the BIP-1 allow a reduction of the gap between implant and bone while resisting to the stumbling forces $F_{stumbling}$ (considered as the worse loading case).

As explain in the introduction section, titanium implants are around nine times stiffer than the bone itself and this difference can cause damages. In the presented test carried out with plastic prosthesis, it has been shown that the process allow a decrease of about 25% in stiffness, from the IP to the BIP-1. Thanks to the force scaling that has been done, these conclusions can be generalized to the titanium prostheses. Finally, with this shape design, the process can help reducing

the stiffness of the implant by 2.25. The implant is now only 6.75 times stiffer than the bone.

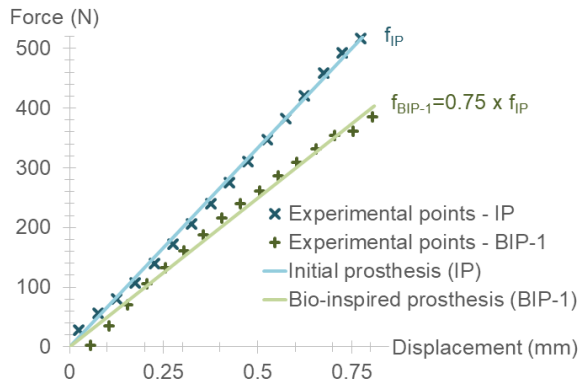

Fig. 5. Plot of the reaction force measured on the dynamometer as a function of the imposed displacement for the IP (blue) and the BIP-1 (green)

3.3.3. FEA on BIP-2

With the two previous sub-section, it has been shown that the local material removal process allows a global decrease of the stiffness of the part. In this sub-section, a second bio-inspired prosthesis (BIP-2) will be investigated numerically. Here will be investigated the influence of the pattern size on the stiffness of the part. For this study, the pattern size p_2 used to remove material to get BIP-2 is smaller than p_1, but also closer to the pattern size originated from the bio-inspired laws. Here, biocompatibility is more taken into account.

The material removal follows the same process as the previously used one (same original part, boundary conditions, material and FEA parameters). For this BIP-2, the pattern size p_2 has been lowered compared to the pattern size p_1. Reducing the pattern size, the ellipses are much smaller and thus the walls are much thinner (too thin to be plastic 3D-printed but thick enough to be metal 3D-printed [11]). For this reason, this geometry will be exclusively investigated through FEA. Numerically, as for BIP-1, BIP-2 is 29% lighter than IP.

The FEA results have shown that for a same applied force and the same amount of removed material, BIP-2 seems to be 2% stiffer than BIP-1. Indeed, the displacements observed on the BIP-2 are 2% smaller than the one of the BIP-1. This difference is due to the difference porosities' size induced by the change of pattern size from p_1 to p_2. Furthermore, it appears that for a same applied force, BIP-2 seems to be 20% softer than the IP (Table 1).

3.4. Discussion

In the introduction section, the stake of reducing the stiffness of the hip prosthesis has been shown. Titanium prostheses have a stiffness nine times bigger than the one of the bone. This difference causes stress shielding and bone delamination issues. Using the material removal process with two different pattern size p_1 and p_2, two parts have been obtained: BIP-1 and BIP-2 (both 29% lighter than IP). With these two designs, the ratio "prosthesis stiffness / bone stiffness" has been reduced from nine to 6.75. This reduction allows a reduction of stress shielding issues by increasing the stresses in the bone surrounding the implant. Mass reduction of the prostheses is also an advantage for the patient that will be able to move easier, increasing its quality of life.

Furthermore, biocompatibility is more considered in the design of bio-inspired prostheses. Indeed, bone porosities are smaller than the one obtained in BIP-1 and trabeculae are thinner. Following this statement, it is shown that biocompatibility is increased for a specific range of porosity sizes. According to some authors, the biocompatibility of the implant is increased when the porosities are bigger than 0.05mm and smaller than 0.8mm [29]. BIP-2 has been designed using a smaller pattern size p_2 closer to the one originated from the bio-inspired laws.

This pattern size p_2 allows the porosities' size to get closer to the recommended range with thinner trabeculae. However, with this smaller pattern size, only 25% of the ellipses have a recommended size. The other 75% of the ellipses are bigger than this range. Thus, the pattern size should be even smaller but it caused issues to compute the CAD model of the bio-inspired prosthesis. Simultaneously, the thinner the trabeculae, the more difficult the manufacturing. Indeed, in the case of plastic 3D-printing, the nozzle of the printer set a minimal printing size that were outreached in the design of BIP-2. However, this geometry may be 3D printed with metallic materials.

Prosthesis	IP	BIP-1	BIP-2
Amount of material (numerical)	Benchmark value	-29%	-29%
Amount of material (printed)	Benchmark value	-31%	/
Displacement (numerical)	0.910 mm	1.161 mm (+28 %)	1.139 mm (+25%)
Stiffness (numerical)	Benchmark value	-22%	-20%
Stiffness (experimental)	Benchmark value	-25%	/
Percentage of ellipses with a biocompatible size	/	0%	25%

Table 1. Summary of the collected data on the three prostheses

Table 1 summarizes the data collected during the previous experiments (from Section 3.3.1 to Section 3.3.3).

It can be noticed that for the same loading and amount of material, the displacement of the BIP-2 is smaller than the BIP-1 one, so that the BIP-2 is stiffer than the BIP-1. Indeed, the smaller the porosities, the more precise their shape and dimension regarding the local stresses. This rise in accuracy entails a smaller decrease of the stiffness of the part.

To summarize, the tested prostheses showed two behaviors:

- The BIP-1, with its bigger ellipses, presents a greater decrease in stiffness (maintaining enough stiffness to resist to the loadings) and present a lower bio-compatibility;
- The BIP-2, with its smaller ellipses, presents a smaller decrease in stiffness (maintaining enough stiffness to resist to the loadings) and present a higher biocompatibility.

Finally, a balance has to be found between the trio {bigger ellipses / stiffness closer to bone stiffness / low

biocompatibility} and {smaller ellipses / stiffness further to bone stiffness / high biocompatibility}. The type of manufacturing technology will also have to be considered.

4. Conclusion

This paper presents a method of material removal bio-inspired from long bone trabecular structure. Material is removed by holing the mechanical part with bio-inspired elliptic holes. Their size and orientation are also bio-inspired following laws presented in previous studies and depend on the stress field in the part. This material removal process has been applied on a hip prosthesis stem.

Hip prostheses are stiffer than the bone they are implanted in (around nine times). This difference of stiffness causes damages on bone and results in implant loosening. To reduce these risks, the stiffness of the implant must be reduced. Using the material removal process, it has been possible to reduce the stiffness of the prosthesis by up to 22%. Instead of having a prosthesis nine times stiffer than the bone, the proposed design obtained using the method is around 6.75 times stiffer than the bone. Other design shown that a balance has to be find by the manufacturer between size of ellipses, stiffness, biocompatibility and manufacturability. To finish with, the process highlighted a mass reduction of 31% that is valuable for patient quality of life.

Acknowledgment

The experimental equipment was funded by the European Community, French Ministry of Research and Education and Aix-Marseille Conurbation Community. Authors aknowledge the Association Nationale Recherche Technologie (France) for financial support through a Convention Industrielle de Formation par la Recherche fund (Cifre thesis n°2020/0881).

Reference

[1] Huiskes HWJ, Vroemen W. A standardized finite element model for routine comparative evaluations of femoral hip prostheses. Acta Orthop. Belg. 1986; 52(3). p. 258-261
[2] Aherwar A, Singh AK, Patnaik A. Current and future biocompatibility aspects of biomaterials for hip prosthesis. AIMS Bio-engng. 2016; 3(1). p. 23-43
[3] Mihov D, Katerska B. Some biocompatible materials used in medical practice. Trakia J. Sci. 2010; 8 (2). p. 119-125
[4] Corona-Castuera J, Rodriguez-Delgado D, Henao J, Castro-Sandoval JC, Poblano-Salas CA. Design and fabrication of a customized partial hip prosthesis employing CT-scan data and lattice porous structures. ASC Omega 2021; 6. p. 6902-6913
[5] Huiskes R, Ruimerman R, van Lenthe GH, Janssen JD. Effects of mechanical forces on maintenance and adaptation of form in trabecular bone. Nature 2000; 405. p. 704-706
[6] Shuib S, Ridzwan MIZ, Hassan AY, Ibrahim MNM. Topology optimisation of hip prosthesis to reduce stress shielding. Comp. Aided Optim. Des. in Engng 2005; IX. p. 257-266
[7] Hamidi E, Fazeli A, Yajid MAM, Sidik NAC, Materials selection for hip prosthesis by the method of weighted properties. Jurnal Teknologi 2015; 75:11
[8] Pizzolato A, Sharma A, Maute K, Sciacovelli A, Verda V. Multi-scale topology optimization of multi-material structures with controllable geometric complexity: Applications to heat transfer problems. Comp. Meth. Appl. Mech. Engng. 2019; 357:112552
[9] Sufiiarov VS, Borisov EV, Sokolova VV, Chukovenkova MO, Soklakov AV, Mikhaluk DS, Popovich AA. Structural analysis of an endoprosthesis designed with graded density lattice structures. Int. J. Numer. Meth. Biomed. Engng. 2021; 37:2
[10] Scerrato D, Bersani AM, Giorgio I, Bio-inspired design of a porous resorbable scaffold for bone reconstruction: a preliminary study. Biomimetics 2021; 6:18
[11] Audibert C, Chaves-Jacob J, Linares JM, Lopez QA. Bio-inspired method based on bone architecture to optimize the structure of mechanical workpieces. Mater. & Des. 2018; 160. p. 708-717
[12] Bilhère-Dieuzeide M, Chaves-Jacob J, Buhon E, Biguet-Mermet G, Linares JM. Stress-driven method bio-inspired by long bone structure for mechanical part mass reduction by removing geometry at macro and cell-unit scales. Mater. & Des. 2022; 213:110318
[13] Frantzl P, Weinkamer R. Nature's hierarchical materials. Prog. Mater. Sci. 2007; 52:8. p. 1263-1334
[14] Giorgio I, Spagnuolo M, Andreaus U, Scerrato D, Bersani AM. In-depth gaze at the astonishing mechanical behavior of bone: a review for designing bioinspired hierarchical materials. Mathe. Mech. Solids 2020; 26:7. p. 1074-1103
[15] Meyers MA, Chen PY, Lin AYP, Seki Y. Biological materials: structure and mechanical properties. Prog. Mater. Sci. 2008; 53:1. p. 1-206
[16] Ruff C, Holt B, Trinkaus E. Who's afraid of the big bad Wolff? : ''Wolff's law'' and bone functional adaptation. Am. J. Phys. Antropol. 2006; 129:4. p. 484-498
[17] Nazarian A, Muller J, Zurakowski D, Muller R, Snyder BD. Densitometric, morphometric and mechanical distribution in the human proximal femur. J. Biomech. 2007; 40:11. p. 2573-2579
[18] Parfitt AM, Drezner MK, Glorieux FH, Kanis JA, Malluche H, Meunier PJ, Ott SM, Recker RR. Bone histomorphometry: standardization of nomenclature, symbols and units. J. Bone Miner. Res. 1987; 2:6. p. 595-610
[19] Harrigan TP, Mann RW. Characterization of microstructural anisotropy in orthotropic materials using a second rank tensor. J. Mater. Sci. 1984; 19. p. 761-767
[20] Doube M, Kłosowski MM, Wiktorowicz-Conroy AM, Hutchinson JR, Shefelbin SJ. Trabecular bone scales allometrically in mammals and birds. Proc. Royal Soc. B 2011; 278:1721. p. 3067-3073
[21] Tsubota KI, Suzuki Y, Yamada T, Hojo M, Makinouchi A, Adachi T. Computer simulation of trabecular remodeling in human proximal femur using largescale voxel FE models: approach to understanding Wolff's law. J. Biomech. 2009; 42:8. p. 1088-1094
[22] Brailneanu PI, Simion I, Bou-Said B, Prisecaru DA, Crisan N. Custom hip stem additive prototyping using smart materials. Mater. Plast. 2020; 57:2. p. 152-158
[23] Ploeg HL, Bürgi M, Wyss UP. Hip stem fatigue test prediction. Int. J. Fatigue 2009; 31. p. 894-905
[24] Nguyen VD, Noels L. Computational homogenization of cellular materials. Int. J. Solids Mater. 2014; 51. p. 2183-2203
[25] Malau DP, Utomo MS, Annur D, Asmaria T, Prabowo Y, Rahyussalim AJ, Supriadi S, Amal MI. Finite element analysis of porous stemmed hip prosthesis for children. AIP Conf. Proc. 2019; 2193:050020
[26] Ikhsan, Prabowo AR, Sohn JM, Triyono J. Finite element analysis of different artificial hip stem designs based on fenestration under static loading. Proc. Struct. Integrity 2020; 27. p. 101-108
[27] Bergmann G, Graichen F, Rohlmann A. Hip joint contact forces during stumbling. Langenbeck's archives surgery 2004; 389. p. 53-59
[28] Colic K, Sedmak A, Grbovic A, Tatic U, Sedmak S, Djordjevic B. Finite element modeling of hip implant static loading. Proc. Engng. 2016; 149. p. 257-262
[29] Arabnejad S, Pasini D. Multiscale design and multiobjective optimization of orthopedic hip implants with functionally graded cellular material. J. Biomech. Engng 2012; 134:3